Migration of multicomponent seismic data using elastic screen method

Xiao-Bi Xie and Ru-Shan Wu, Institute of Geophysics and Planetary Physics, University of California, Santa Cruz, CA 95064*

Summary

A complex screen propagator for elastic waves is used in multicomponent seismic migration and imaging. Imaging conditions for both P-P imaging and P-S converted wave imaging are proposed to handle polarizations of the data. The propagators and imaging conditions are tested with numerical examples.

Introduction

Multicomponent data increased the information of seismic data. Recent developments of ocean bottom seismic (OBS) technology make more multicomponent data available. From these data, both P-P and P-S sections can be obtained. Since these waves carry different properties of the target reflectors, combining them together can provide us with petrophysical parameters that cannot be obtained with P-wave data alone. However, extracting the new information requires more physically rigorous techniques.

Many attempts have been made to carry out elastic wave migrations. Chang and McMechan (1987, 1994) conducted 2D and 3D elastic reverse-time migrations using a full wave finite-difference method. Zhe and Greenhalgh (1997) used potentials, instead of displacements, to propagate P and S waves. Hokstad (2000) proposed a multicomponent Kirchhoff migration method and a specially designed imaging condition for multicomponent elastic waves. On the other hand, others chose to treat elastic waves as scalar waves with different speeds and used scalar wave propagator to do the migration. Using scalar wave propagators to simulate elastic wave propagation, although straightforward, sometimes over simplifies the real physical processes.

On the other hand, the phase screen method for scalar wave migration has been used for many years (Stoffa et al., 1990). Several modifications of this method have been made to improve its accuracy under wide-angle and large velocity contrasts (e.g., Ristow and Ruhl, 1994; Jin, et al., 1998; Xie and Wu, 1998; Huang, et al., 1999; Huang and Fehler, 2000; Xie et al., 2000). Compared with other methods, this one-way wave equation based method provided an efficient, high quality propagator for scalar wave migration. The scalar wave screen propagator has also been extended into elastic wave case (Wu, 1994, 1996; Xie and Wu, 1996, 2000; Wild and Hudson ,1998). Wu and Xie (1994) did some primary work to test the elastic screen method as a backpropagator for multi-component elastic migration.

Based on the above-mentioned progresses, it is natural to extend the scalar wave screen migration method to the multicomponent elastic wave case. In the following sections, we propose an elastic screen propagator and vector imaging conditions for prestack depth migration and imaging of multicomponent seismic data.

Screen Propagator for Elastic Waves

Based on the one-way wave equation and scattering theory, the screen solution of a forward propagating elastic wave passing through an inhomogeneous thin slab between z_0 and z_1 can be represented as a superposition of plane P and S waves

$$\mathbf{u}(\mathbf{x}_T, z_1) = \frac{1}{4\pi^2}\int d\mathbf{K}_T \times[\mathbf{u}^P(\mathbf{K}_T, z_1) + \mathbf{u}^S(\mathbf{K}_T, z_1)]e^{i\mathbf{K}_T\cdot\mathbf{x}_T} \quad (1)$$

where $\mathbf{K}_T$ is the transverse wavenumber of plane waves, $\mathbf{x} = \mathbf{x}_T + z$ is the position vector, superscripts P and S denote P and S waves, and

$$\mathbf{u}^P(\mathbf{K}_T, z_1) = e^{i\gamma_\alpha \Delta z}[\mathbf{u}_0^P(\mathbf{K}_T, z_0) + \mathbf{U}^{PP}(\mathbf{K}_T, z_0) + \mathbf{U}^{SP}(\mathbf{K}_T, z_0)] \quad (2)$$

$$\mathbf{u}^S(\mathbf{K}_T, z_1) = e^{i\gamma_\beta \Delta z}[\mathbf{u}_0^S(\mathbf{K}_T, z_0) + \mathbf{U}^{SS}(\mathbf{K}_T, z_0) + \mathbf{U}^{PS}(\mathbf{K}_T, z_0)] \quad (3)$$

where $\Delta z = z_1 - z_0$, γ_α and γ_β are vertical wave-numbers for P and S waves, $\mathbf{u}_0$ is the incident wave, $\mathbf{U}^{PP}$, $\mathbf{U}^{SP}$, $\mathbf{U}^{SS}$ and $\mathbf{U}^{PS}$ are different types of scattered waves. Detailed expressions of these scattered fields can be found in Xie and Wu (1996, 2000). These equations formed the basis of elastic screen propagator. For elastic wave seismic migration, we have to propagate down going waves from the source to the target and backpropagate reflected waves from the receiver to the target. If the coupling between P and S waves can be neglected along the entire propagation leg (other than the target reflector), we may choose either $\mathbf{u}^P$ or $\mathbf{u}^S$ in equation (1) to form a single wave type propagator. $\mathbf{U}^{SP}$ and $\mathbf{U}^{PS}$ in equations (2) and (3) can also be neglected. Using Rytov approximation, equations (2) and (3) can be rewritten as (Wu and Xie, 1994; Xie and Wu, 1996, 2000)

$$\mathbf{u}^P(\mathbf{K}_T,z_1)=e^{i\gamma_\alpha\Delta z}\int d\mathbf{x}'_T e^{-i\mathbf{K}_T\cdot\mathbf{x}'_T}\times\mathbf{u}_0^P(\mathbf{x}'_T,z_0)e^{-ik_\alpha\Delta z\delta\alpha/\alpha_0} \quad (4)$$

$$\mathbf{u}^S(\mathbf{K}_T,z_1)=-e^{i\gamma_\beta\Delta z}\hat{k}_\beta\times\Big[\hat{k}_\beta\times\times\int d\mathbf{x}'_T e^{-i\mathbf{K}_T\cdot\mathbf{x}'_T}\mathbf{u}_0^S(\mathbf{x}'_T,z_0)e^{-ik_\beta\Delta z\delta\beta/\beta_0}\Big] \quad (5)$$

Equations (4) and (5), together with equation (1), form single wave type propagators for P and S waves. For back propagation, the conjugates of these propagators can be used. Alternatively, one can choose to use the forward propagator together with time-reversed data (or equivalently, the conjugate of the frequency domain data) to conduct a back propagation. The advantage of the later is one propagator can be used for both down and up going waves (in case both of them are in the same wave type).

The above equations are derived based on small perturbation theory. For large velocity contrasts and wide scattering angles, the modification method proposed by Xie and Wu (1999) can be adopted to improve the accuracy.

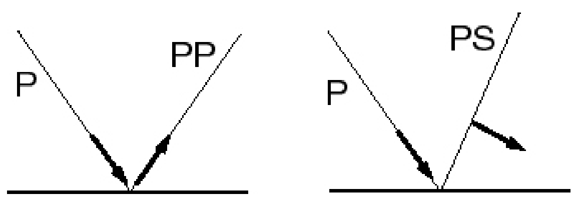

Figure 1. Sign conventions for polarizations. The P-P and P-S polarizations shown in this figure correspond to positive impedance changes.

Imaging Conditions

Based on the scattering theory and omitting the angle related factors, the reflected P-P wave from an interface can be related to the model as (Xie and Wu, 1996, 2000; Wild and Hudson, 1998)

$$u^{PP}(\mathbf{x}_T)\sim u_0^P(\mathbf{x}_T)\frac{\Delta Z_\alpha(\mathbf{x}_T)}{Z_{\alpha 0}}. \quad (6)$$

Similarly, for P-S converted wave we have

$$u^{PS}(\mathbf{x}_T)\sim u_0^P(\mathbf{x}_T)\times\left[\frac{\Delta Z_\beta(\mathbf{x}_T)}{Z_{\beta 0}}+\left(\frac{\beta_0}{\alpha_0}-\frac{1}{2}\right)\frac{\Delta\mu(\mathbf{x}_T)}{\mu_0}\right]. \quad (7)$$

where u_0^P is the amplitude of incident P wave, u^{PP} and u^{PS} are amplitudes of reflected P and S waves from the interface. $\Delta Z_\alpha/Z_{\alpha 0}$ and $\Delta Z_\beta/Z_{\beta 0}$ are fractional P and S wave impedance changes across the interface, $\Delta\mu/\mu_0$ is the fractional shear modular change. Above equations reveal that the reflected P-P wave carries the P wave impedance information while the P-S converted wave mainly carries the S wave impedance information. More petrophysical parameters can be obtained by combining both P wave and converted wave information. Following Mittet et al. (1995), the imaging conditions for P and converted waves can be constructed as

$$I^{PP}(\mathbf{x}_T,z)=\int C^{PP}u_0^P(\mathbf{x}_T,z,\omega)u^{PP}(\mathbf{x}_T,z,\omega)^* d\omega \quad (8)$$

$$I^{PS}(\mathbf{x}_T,z)=\int C^{PS}u_0^P(\mathbf{x}_T,z,\omega)u^{PS}(\mathbf{x}_T,z,\omega)^* d\omega \quad (9)$$

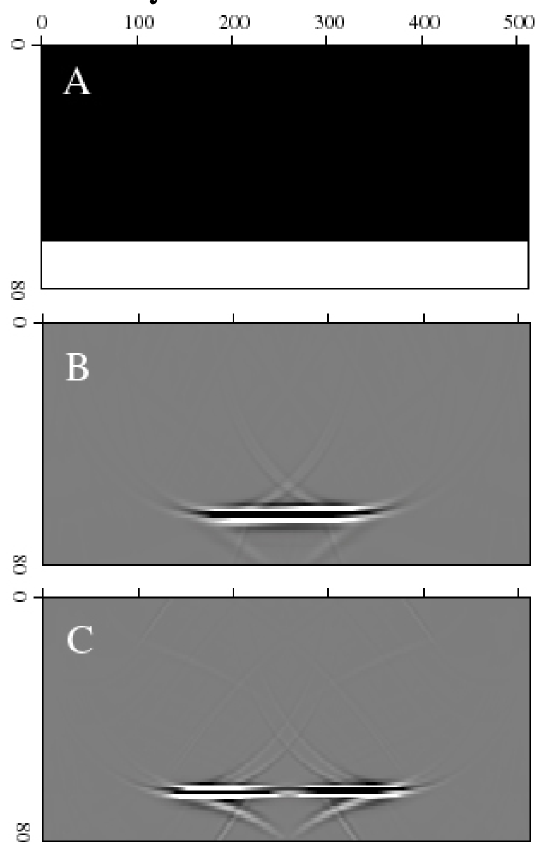

Figure 2. Single shot prestack imaging. A: velocity model, B: P-wave image and C: converted wave image.

where u_0^P is the amplitude of down going P wave from the source, u^{PP} and u^{PS} are amplitudes of back propagated up going P and S waves from receivers. C^{PP} and C^{PS} are normalization factors. Mittet et al. (1995) discussed several different normalizations. Here we chose their simplest form but added proper sign conventions to handle polarizations. An imaging process is basically recovering properties of an interface with incident and scattered waves. These properties should not depend on the coordinate system chosen to conduct the numerical calculations. For this reason, we define a "positive" impedance interface if the incident and scattered waves take the same polarizations as shown in Figure 1. Based on equations (6) and (7), these imaging conditions should generate images reflecting different properties of the model.

Numerical Examples

The elastic wave propagator and imaging conditions are tested with numerical examples. The first example is a simple two-layer model with a flat interface. Shown in Figure 2A is the velocity model. The velocities and densities are α_1=3.5 km/s, β_1=2.0 km/s, ρ_1=2.0 g/cm^3, and α_2=4.5 km/s, β_2=2.4 km/s, ρ_2=2.2 g/cm^3, respectively. The size of the model is 5.12 km in horizontal and 1.6 km in vertical direction. A single shot is located in the center of the surface. Synthetic seismograms are generated using an elastic finite-difference method (Xie and Lay, 1994). 350 receivers are located on the surface. Elastic screen propagator is used for both down going P-wave and up going P-P and P-S waves. Vector imaging conditions are applied to obtain the P wave and converted wave images. For calculating synthetic seismograms, dx = dz = 5 m and dt = 0.5 ms are used. For migration, we use dx = 10 m, dz = 20 m and dt = 4 ms. The receiver space is 10 m.

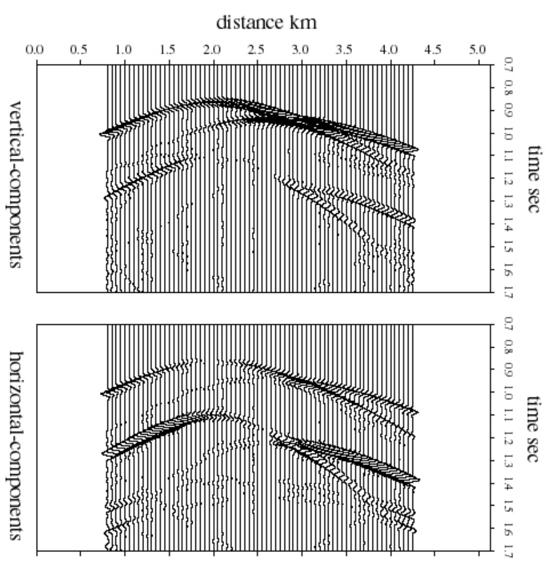

Figure 3. Synthetic shot record for model shown in Figure 4A. First arrivals have been removed from the record.

Shown in Figures 2B and 2C are P-P image and P-S converted wave image. Several features can be seen from this simple model. Since the S-wave incident angle is smaller than that of the P-wave, the P-S image has a wider angle coverage. In other words, under the same source-receiver configuration, converted wave provides a better illumination of the targets. With the application of vector imaging conditions, the converted wave image has the correct polarization on both sides of the source. This allows us to construct the image by stacking results from multiple shots. Due to the shorter wavelength of the S wave, the resolution of the P-S image is slightly better than the P-P image.

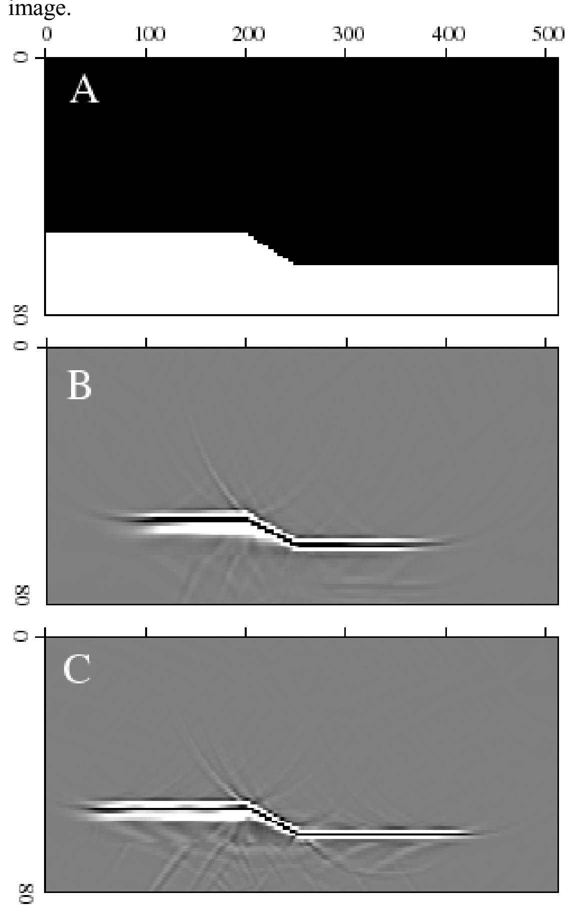

Figure 4. Prestack image for a step interface. A: velocity model, B: P-wave image and C: converted wave image. Partial images from four shots are stacked together to generate this image.

The second example is also a two-layer model but with an interface that simulates a fault. The velocity model is shown in Figure 4A. The velocity and density parameters are similar to that used in the first example. Four shots on the surface (at grid points 150, 200, 250 and 300) are used to illuminate the structure. A typical common shot gather is shown in Figure 3. Note that for larger offsets the converted waves are rather prominent, especially on horizontal components. The stacked P-P image and P-S converted wave image are shown in Figures 4B and 4C. Benefitting from vector image condition, the converted wave image can be easily stacked together. Although only four shots are used, qualities for both P-wave and converted wave images are good.

Discussion and Conclusion

The elastic complex screen method based on the one-way wave equation is used for multicomponent seismic migration. Vector imaging conditions for both P-P wave imaging and P-S converted wave imaging are also proposed. The scalar wave treatment of the converted wave is simple and easy to perform. However, it lost many useful dynamic properties of elastic waves. Compared with the scalar wave treatment, true elastic wave propagators and vector imaging conditions preserve more dynamic properties in the propagation and imaging processes. It is expected that petrophysical parameters can be better extracted using multicomponent migration/imaging. The vectorized imaging condition also solves the polarization problem and makes stacking multi-shot converted wave images straightforward. Limited by the current space domain imaging condition, obtained images are weighted averages of reflectivities from mixed incident angles. To obtain angle related information, a wavenumber domain imaging condition may be required.

References

Chang, W.F. and McMechan, G.A., 1987, Elastic reverse-time migration, Geophysics, 52, 1367-1375.

Chang, W.F. and McMechan, G.A., 1994, 3-D elastic prestack reverse-time depth migration, Geophysics, 59, 597-609.

Hokstad, K., 2000, Multicomponent Kirchhoff migration, Geophysics, 65, 861-873.

Huang, L.J. and Fehler, M.C., 2000, Globally optimized Fourier finite-difference migration method, Expanded Abstracts, SEG 70th Annual Meeting, 802-805.

Huang, L.J., Fehler, M.C. and Wu, R.S., 1999, Extended local Born Fourier migration method, Geophysics, 64, 1524-1534.

Jin, S., Wu, R.S. and Peng, C., 1998, Prestack depth migration using a hybrid pseudo-screen propagator, Expanded Abstracts, SEG 68th Annual Meeting, 1819-1822.

Mittet, R., Sollie, R. and Hokstad, Ketil, 1995, Prestack depth migration with compensation for absorption and dispersion, Geophysics, 1485-1494.

Ristow, D. and Ruhl, T, 1994, Fourier finite-difference migration, Geophysics, 59, 1882-1893.

Stoffa, P.L., Fokkema, J.T., Freire, R.M.D., and Kessinger, W.P., 1990. Split-step Fourier migration, Geophysics, 55, 410-421.

Wild, A.J. and Hudson, J.A., 1998, A geometrical approach to the elastic complex screen, J. Geophys. Res., 103, 707-725.

Wu, R.S., 1994, Wide-angle elastic wave one-way propagation in heterogeneous media and an elastic wave complex-screen method, J. Geophys. Res., 99, 751-766.

Wu, R.S., 1996, Synthetic seismograms in heterogeneous media by one-return approximation, Pure and Applied Geophys., 148, 155-173.

Wu, R.S. and Xie, X.B., 1994, Multi-screen back propagator for fast 3D elastic prestack migration, SPIE.

Xie, X.B. and Lay, T., 1994, The excitation of Lg waves by explosions: A finite-difference investigation, Bull. Seism. Soc. Am., 84, 324-342.

Xie, X.B. and Wu, R.S., 1996, 3D elastic wave modeling using the complex screen method, Expanded Abstracts of the Technical Program, SEG 66 th Annual Meeting, 1247-1250.

Xie, X.B. and Wu, R.S., 1998, Improve the wide angle accuracy of screen method under large contrast, Expanded abstracts, SEG 68th Annual Meeting, 1247-1250.

Xie, X.B. and Wu, R.S., 1999, Improve the wide angle accuracy of the screen propagator for elastic wave propagation, Expanded Abstracts, SEG 69th Annual Meeting, 1863-1866.

Xie, X.B., Mosher, C.C. and Wu, R.S., 2000, The application of wide angle screen propagator to 2D and 3D depth migrations, Expanded Abstracts, SEG 70th Annual Meeting, 878-881.

Xie, X.B. and Wu, R.S., 2000, modeling elastic wave forward propagation and reflection using the complex screen method, submitted to JASA.

Zhe, J. and Greenhalgh, S.A., 1997, Prestack multi-component migration, Geophysics, 62, 598-613.